Complex-Regge-Pole Model in πN Scattering*

Robert T. Park†
California State University, Northridge, California 91324
and University of California, Riverside, California 92502
and
N. Barik‡
University of California, Riverside, California 92502
and
David T. Gregorich
California State University, Los Angeles, California 90032
(Received 31 July 1972)

The complex-Regge-pole model is applied to πN elastic and charge-exchange scattering in the forward direction. P, P', and ρ poles are assumed to dominate with both square-root and logarithmic singularity at the branch point. The Pomeranchuk trajectory is parametrized both as a real pole and as a pair of complex-conjugate poles. Various ghost-eliminating mechanisms are tested, and good fits are obtained including excellent agreement with the new πN charge-exchange and elastic polarization data. P' and ρ are nearly exchange degenerate, but the data show no strong preference for either a real or complex Pomeranchuk trajectory or for a square-root or logarithmic branch cut.

I. INTRODUCTION

In recent years Regge-cut models have played an increasingly important role in the description of high-energy scattering data. In the complex-Regge-pole (CRP) model the cut contribution is approximated by complex Regge poles so that the entire scattering amplitude may be expressed as a sum over complex poles. This model has been very successful in fitting a wide range of scattering processes, and in particular successful fits have been obtained to the πN charge-exchange data.[1,2] These fits were characterized by positive, nonzero charge-exchange polarization and a crossover zero in the imaginary part of the spin-nonflip amplitude. The crossover zero in $\mathrm{Im}A'$ was accomplished without introducing a zero simultaneously into $\mathrm{Re}A'$, and thus the usual contradictions of the factorization hypothesis were avoided.

In view of the success of these earlier CRP fits in πN charge-exchange scattering, we have extended the results to πN elastic scattering as well. In the analysis we were interested in the following details:

(1) Existence of new polarization data. The work of Guisan *et al.*[3] has provided new charge-exchange polarization data for larger values of $-t$, and Borghini *et al.* have obtained $\pi^- p$ and $\pi^+ p$ elastic polarization values[4] which extend to larger $-t$ and are much more complete than previous data. The new data place strong restrictions on phenomenological models, and it is of interest to test the success of the CRP model in fitting these data.

(2) Crossover zero and simultaneous fitting of all data. In a simultaneous fit of the πN elastic and charge-exchange data the crossover phenomenon can be studied directly, and one can determine the precise relationship between the zero in $\mathrm{Im}A'$ and the crossover of the $\pi^- p$ and $\pi^+ p$ elastic differential cross sections. Also, the ρ parameters which are consistent with *both* the elastic and charge-exchange data can be obtained.

(3) Nature of the Pomeranchuk trajectory. The Pomeranchuk trajectory is parametrized both as a real pole and as a pair of complex-conjugate poles, and we shall include here a brief discussion of the parametrization with complex-conjugate poles.

It is now well established theoretically that complex-conjugate Regge poles exist for $t \leq 0$ if cuts in the j plane also exist.[5] In this case the scattering amplitude is represented by an integral over the branch cut plus a pair of complex-conjugate Regge poles, if the poles are on the physical sheet, and by the cut integral alone when the poles are on the unphysical sheet. However, the Pomeranchuk trajectory has the following special property. If it is present as a pair of complex-conjugate poles, then either the poles are on the unphysical sheet or $\mathrm{Im}\alpha$ vanishes at $t=0$. Otherwise, total cross sections would become negative at asymptotic energies.

Ball, Marchesini, and Zachariasen (BMZ) have shown that the cut integral, at intermediate energies and small values of $\mathrm{Im}\alpha$, can be approximated

by complex-conjugate poles.[6] This approximation is expected to hold for a complex Pomeranchuk trajectory in the same way as for other complex Regge poles. Thus, at intermediate energies and small Imα, the entire scattering amplitude may be parametrized with complex-conjugate poles including the Pomeranchuk trajectory.

Because the BMZ approximation fails at very high energies, where it is necessary to calculate the behavior of the cut integral directly, we have restricted the maximum value of p_{lab} in the experimental data to about 30 BeV/c. Within this range we wish to determine whether the data show a preference for either a real or complex-conjugate Pomeranchuk trajectory.

(4) Type of branch point singularity. Cut models involving both logarithmic and square-root singularities at the branch point have been proposed, and we attempt to determine which is superior.

(5) Behavior of complex trajectories. It is of interest to determine more precisely the parameters of the ρ and P' trajectories in the CRP model and to test the hypothesis of ρ-P' exchange degeneracy.

(6) Models for the residues. Different models for the $I=0$ residue functions are used including the Barger-Phillips cyclic residue,[7] the Chew mechanism,[8] and the no-compensation mechanism.[9]

II. πN AMPLITUDES AND THE COMPLEX-REGGE-POLE MODEL

Regge trajectories P, P', and ρ are assumed to dominate the t-channel exchange. In what follows, the Pomeranchuk trajectory is parametrized as a pair of complex-conjugate poles. The appropriate modifications for a real Pomeranchuk trajectory will be discussed later.

The πN invariant amplitudes $A'(s,t)$ and $B(s,t)$ for individual P, P', and ρ exchange are parametrized as follows:

$$A'(s,t)=\gamma_{+A}\left(\frac{\nu}{\nu_0}\right)^{\alpha_+}\xi(\alpha_+)+\gamma_{-A}\left(\frac{\nu}{\nu_0}\right)^{\alpha_-}\xi(\alpha_-), \tag{1}$$

$$B(s,t)=\gamma_{+B}\left(\frac{\nu}{\nu_0}\right)^{\alpha_+-1}\xi(\alpha_+)+\gamma_{-B}\left(\frac{\nu}{\nu_0}\right)^{\alpha_--1}\xi(\alpha_-), \tag{2}$$

where

$$\nu=E_{\text{lab}}+\frac{t}{4m_N}\quad\text{and}\quad\nu_0=1\ \text{BeV} \tag{3}$$

and the signature factor $\xi(\alpha)$ is given by

$$\xi(\alpha)=\frac{\pm1-e^{-i\pi\alpha}}{\sin\pi\alpha}. \tag{4}$$

The plus sign in (4) corresponds to ρ exchange, and the minus sign to P and P' exchange.

We may express the amplitudes for π^-p and π^+p elastic scattering and π^-p charge-exchange (CEX) scattering in terms of the amplitudes for exchange of individual trajectories

$$A'_{\pi^-p}=A'_P+A'_{P'}+A'_\rho, \tag{5}$$

$$A'_{\pi^+p}=A'_P+A'_{P'}-A'_\rho, \tag{6}$$

$$A'_{\text{CEX}}=-\sqrt{2}\,A'_\rho, \tag{7}$$

TABLE I. High-energy scattering data used in the fits.

Measurement	Values of p_{lab} (BeV/c)	No. of data points	References
$\frac{d\sigma}{dt}(\pi^-p\to\pi^0n)$	5.85, 9.8, 13.3, 18.2	57	10
$P(\pi^-p\to\pi^0n)$	5.0, 5.9, 8.0, 11.2	27	3, 11
$\sigma_{\text{total}}(\pi^\pm p)$	7–29	24	12
$\alpha(\pi^\pm p)=\frac{\text{Re}A'(\pi^\pm p)}{\text{Im}A'(\pi^\pm p)}\Big\vert_{t=0}$	7–27	20	13
$\frac{d\sigma}{dt}(\pi^+p\to\pi^+p)$	6.8, 12.4, 16.7	47	14
$\frac{d\sigma}{dt}(\pi^-p\to\pi^-p)$	6.0, 10.8, 15.0, 18.4	63	14, 15
$P(\pi^+p\to\pi^+p)$	6.0, 10.0, 12.0, 17.5	58	4, 16
$P(\pi^-p\to\pi^-p)$	6.0, 10.0, 14.0	62	4
	Total data points	358	

TABLE II. Values of χ^2 in the cyclic residue model for the data in Table I.

Branch-point singularity	Real Pomeranchuk trajectory	Complex Pomeranchuk trajectory
Square-root	952	761
Logarithmic	895	1154

and similarly for the B amplitudes. The formulas for cross sections and polarization can be found in Ref. 8.

The trajectories in the CRP model are of two types, corresponding to the nature of the branch-point singularity. For a logarithmic cut we write

$$\alpha_\pm = a + bt \pm ig \tag{8}$$

and for the square-root cut

$$\alpha_\pm = a + bt \pm ig(-t)^{1/2}. \tag{9}$$

The Pomeranchuk trajectory has $a=1$ in all cases.

The residues for the ρ trajectory are parametrized as follows:

$$\gamma_{+A} = \gamma^*_{-A} = h_0 e^{h_1 t}(\alpha_+ + 1)e^{i\phi_A}, \tag{10}$$

$$\gamma_{+B} = \gamma^*_{-B} = d_0 e^{d_1 t}\alpha_+(\alpha_+ + 1)e^{i\phi_B}, \tag{11}$$

with

$$\phi_A = \pi(\gamma_0 + \gamma_1 t) \quad \text{and} \quad \phi_B = \pi(\lambda_0 + \lambda_1 t) \tag{12}$$

for a logarithmic cut and

$$\phi_A = \pi(-t)^{1/2}(\gamma_0 + \gamma_1 t)$$

and (13)

$$\phi_B = \pi(-t)^{1/2}(\lambda_0 + \lambda_1 t)$$

for a square-root cut.

For the P and P' residues several possibilities are considered. In one case the residues are similar to those used by Barger and Phillips, the cyclic-residue model,[7]

$$\gamma_{+A} = \gamma^*_{-A} = h_0 e^{h_1 t}\sin^2(\tfrac{1}{2}\pi\alpha_+)e^{i\phi_A}, \tag{14}$$

$$\gamma_{+B} = \gamma^*_{-B} = d_0 e^{d_1 t}\sin^2(\tfrac{1}{2}\pi\alpha_+)e^{i\phi_B}, \tag{15}$$

where ϕ_A and ϕ_B are given by Eq. (12) for a logarithmic cut and Eq. (13) for a square-root cut. As a second example, a parametrization similar to that of Rarita *et al.*, the Chew mechanism,[8] is used. In this parametrization $\sin^2(\frac{1}{2}\pi\alpha_+)$ in Eq. (14) is replaced by $\alpha_+(\alpha_+ + 1)$, and $\sin^2(\frac{1}{2}\pi\alpha_+)$ in Eq. (15) is replaced by $\alpha_+^2(\alpha_+ + 1)$. We also test the no-compensation mechanism, where $\sin^2(\frac{1}{2}\pi\alpha_+)$

TABLE III. Parameter values for the cyclic residue model. We have expressed the parameter values in units such that $\hbar = c = 1$, BeV = 1. For the Pomeranchuk trajectory the parameter a has a fixed value of 1 in all fits.

Trajectory	a	b	g	h_0	h_1	d_0	d_1	γ_0	γ_1	λ_0	λ_1
(a) Real Pomeranchuk trajectory, square-root branch cut, cyclic residue.											
P	1	0.18	···	53.9	2.88	−4.86	1.73	···	···	···	···
P'	0.52	0.96	0.21	35.9	1.14	9.67	0.96	0.52	0.56	−0.86	0.01
ρ	0.57	0.90	0.16	1.98	−0.93	34.9	0.71	−1.14	−0.26	−0.50	−0.45
(b) Complex Pomeranchuk trajectory, square-root branch cut, cyclic residue. This is the best fit.											
P	1	0.03	0.13	27.5	2.81	6.38	1.73	0.38	0.18	−1.15	−0.30
P'	0.50	0.91	0.13	36.2	1.09	28.2	1.07	0.01	0.14	−0.76	0.00
ρ	0.57	0.88	0.16	2.03	−0.99	34.8	0.86	−1.13	−0.25	−0.43	−0.43
(c) Real Pomeranchuk trajectory, logarithmic branch cut, cyclic residue.											
P	1	0.26	···	56.7	2.92	−7.02	0.63	···	···	···	···
P'	0.52	0.95	0.10	45.4	1.20	13.9	0.03	0.14	0.02	−0.46	0.59
ρ	0.50	0.89	0.10	−4.47	0.04	65.5	0.94	0.58	0.53	−0.44	−0.24
(d) Complex Pomeranchuk trajectory, logarithmic branch cut, cyclic residue.											
P	1	0.24	0.09	29.0	2.64	−0.13	−0.47	−0.28	−0.01	0.28	−1.19
P'	0.51	1.05	0.13	53.4	1.30	7.29	−0.99	−0.16	0.08	−0.07	0.51
ρ	0.51	0.88	0.10	−3.62	−0.05	50.1	0.54	0.63	0.67	−0.33	−0.16

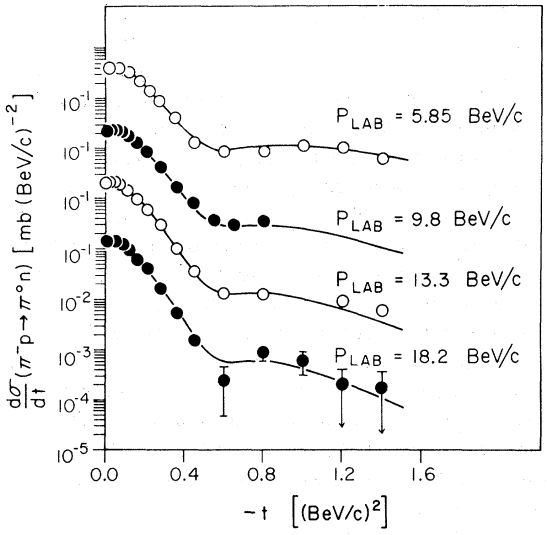

FIG. 1. Theoretical curves for the best fit (cyclic residue, complex Pomeranchuk trajectory, square-root branch cut) to the $\pi^- p$ charge-exchange differential cross section. Data from Ref. 10.

in Eqs. (14) and (15) is replaced by $\alpha_+^2(\alpha_+ + 1)$.

For a real Pomeranchuk trajectory the Pomeranchuk amplitudes are parametrized as follows (in the cyclic residue case):

$$A'(s,t) = \gamma_A \left(\frac{\nu}{\nu_0}\right)^{\alpha} \xi(\alpha), \tag{16}$$

$$B(s,t) = \gamma_B \left(\frac{\nu}{\nu_0}\right)^{\alpha - 1} \xi(\alpha), \tag{17}$$

with

$$\alpha = 1 + bt, \tag{18}$$

$$\gamma_A = h_0 e^{h_1 t} \sin^2(\tfrac{1}{2}\pi\alpha), \tag{19}$$

$$\gamma_B = d_0 e^{d_1 t} \sin^2(\tfrac{1}{2}\pi\alpha). \tag{20}$$

III. DATA AND RESULTS

The high-energy scattering data used in this analysis are taken from Refs. 3, 4, and 10–16 and are listed in Table I. These include $(d\sigma/dt)(\pi^- p \to \pi^0 n)$, $P(\pi^- p \to \pi^0 n)$, $\sigma_{\text{total}}(\pi^\pm p)$, $\alpha(\pi^\pm p)$, $(d\sigma/dt)(\pi^\pm p \to \pi^\pm p)$, and $P(\pi^\pm p \to \pi^\pm p)$, with a total of 358 points.

In Table II we give the values of χ^2 for the best fits to this data in the cyclic-residue case, Eqs. (14) and (15). The results include both a real and complex-conjugate Pomeranchuk trajectory and square-root and logarithmic singularities at the branch point. The corresponding parameter values are given in Table III. We shall present the results for the Chew and no-compensation mechanisms later.

The best fits to the data were obtained for the cyclic residue model with a complex-conjugate Pomeranchuk trajectory and square-root singularity at the branch point – the $\chi^2 = 761$ case. The

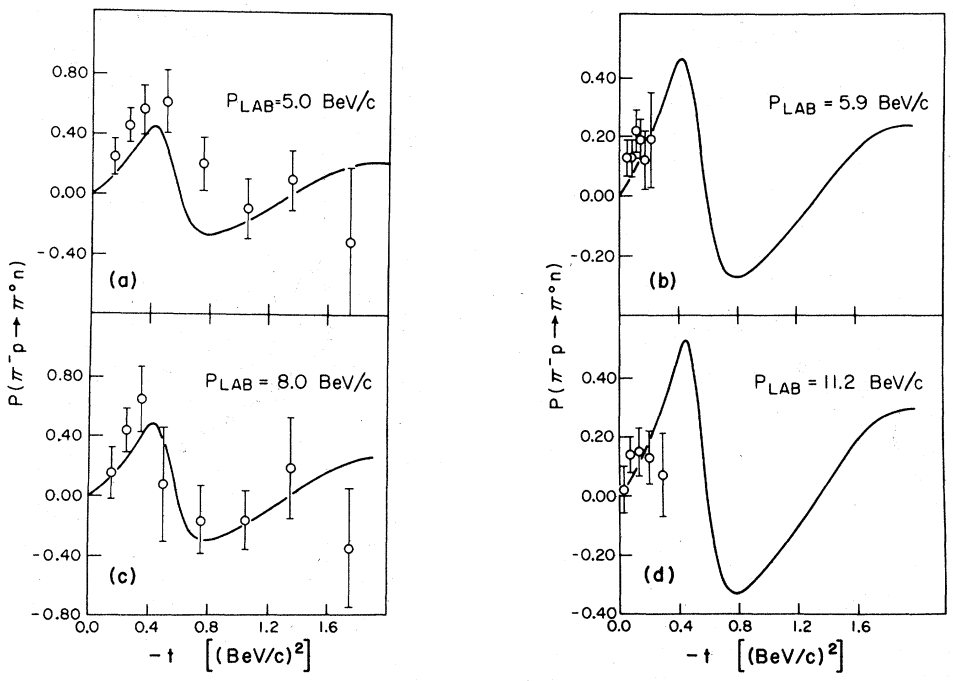

FIG. 2. Fits to the $\pi^- p$ charge-exchange polarization data for (a) $p_{\text{lab}} = 5.0$ BeV/c, (b) 5.9 BeV/c, (c) 8.0 BeV/c, and (d) 11.2 BeV/c. Data from Refs. 3 and 11.

fits in this case[17] are shown in Figs. 1–5. The χ^2 value and quality of fit for charge-exchange scattering, Figs. 1 and 2, are very good and are comparable to Refs. 1 and 2, as we should expect. The results of the fits to the elastic scattering data, Figs. 4 and 5, are also good and are comparable to previous work.[7-9,18-21]

IV. DISCUSSION

We shall divide the discussion into several parts:

(1) Comparison of trajectory and residue models. In Table II we observe some variation in χ^2 values for different cases involving a real and a complex Pomeranchuk trajectory and logarithmic and square-root branch cuts. We do not regard these differences in χ^2 as significant and feel that in the CRP model using the current parametrization the data are not able to distinguish either the type of singularity at the branch point or whether the Pomeranchuk trajectory is real or complex-conjugate. Our reasons are these. First, the graphs of fits to the data for each of the four cases do not show significant differences in over-all quality even when the $\chi^2 = 761$ case is compared with the $\chi^2 = 1154$ case. Secondly, the main qualitative features of the data, for example, the existence of a dip in the charge-exchange differential cross section, are successfully fitted in all four cases. Finally, data are not sufficiently accurate nor is the theory sufficiently well developed to judge the quality of different fits on the basis of small or even intermediate differences in χ^2.

We compared our fits to the data using the cyclic residue model with the fits using the Chew and no-compensation mechanisms. This comparison was made on the basis of a reduced data set with about 100 representative points. The fits for the cyclic residue model have a slightly better value of χ^2 than for the Chew and no-compensation mechanisms. However, the quality of the fits is about the same for all three cases with the exception of the elastic polarization data for which the cyclic residue model is slightly superior. All three cases are in reasonable agreement with the data.

(2) Properties of the trajectories. From Table

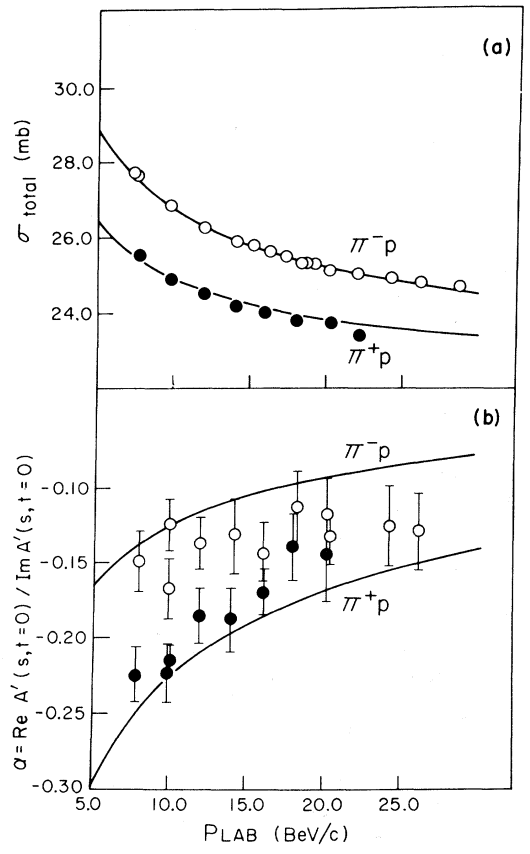

FIG. 3. Fits to (a) π^+p and π^-p total cross sections and to (b) $\alpha(\pi^+p)$ and $\alpha(\pi^-p)$, the phase of the forward amplitude for π^+p and π^-p elastic scattering. Data from Refs. 12 and 13.

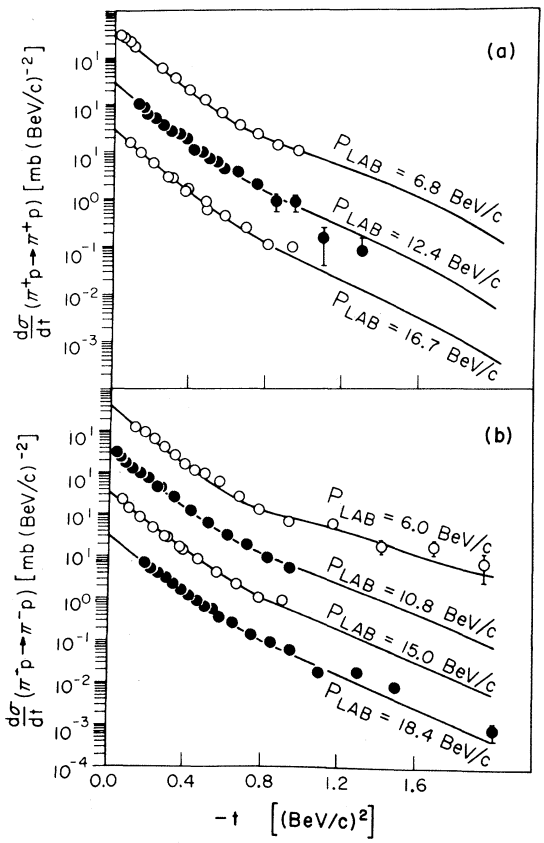

FIG. 4. Theoretical curves and data for (a) $(d\sigma/dt)(\pi^+p \to \pi^+p)$ and (b) $(d\sigma/dt)(\pi^-p \to \pi^-p)$. Data from Refs. 14 and 15.

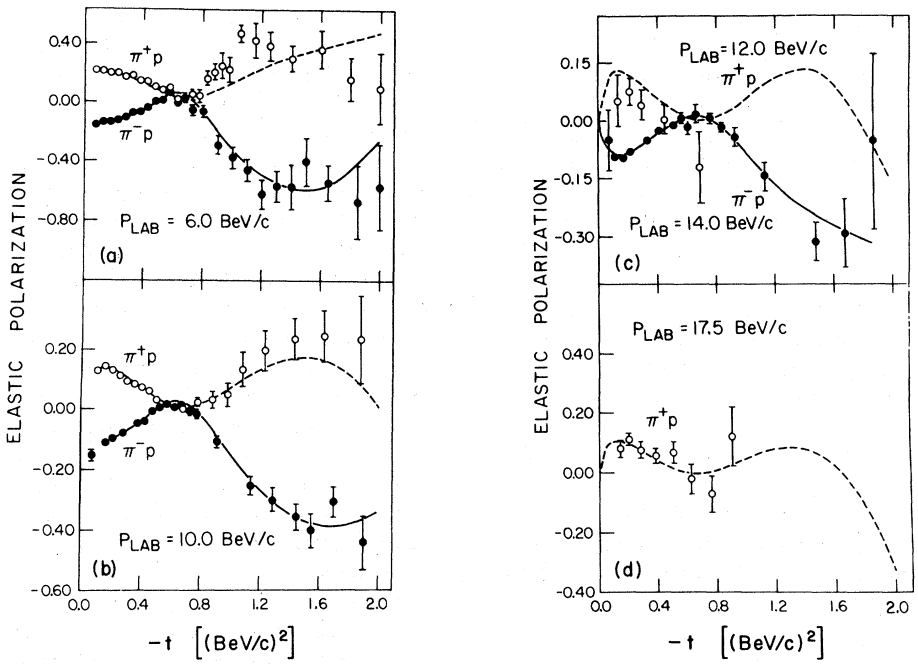

FIG. 5. Fits to the elastic polarization data as follows: (a) π^+p and π^-p at $p_{\rm lab}=6$ BeV/c, (b) π^+p and π^-p at $p_{\rm lab}=10$ BeV/c, (c) π^+p at $p_{\rm lab}=12$ BeV/c and π^-p at $p_{\rm lab}=14$ BeV/c, and (d) π^+p at $p_{\rm lab}=17.5$ BeV/c. Data from Refs. 4 and 16.

III the trajectories for the best fit, $\chi^2=761$, were

$$\alpha_\rho = 0.57 + 0.88t + 0.16(-t)^{1/2}i, \tag{21}$$

$$\alpha_{\rho'} = 0.50 + 0.91t + 0.13(-t)^{1/2}i, \tag{22}$$

$$\alpha_P = 1 + 0.03t + 0.13(-t)^{1/2}i. \tag{23}$$

Except for the slope of the Pomeranchuk trajectory which is smaller in the $\chi^2=761$ case, the parameter values here are comparable to other parameter values in Table III. The ρ parameters for the best fit agree quite closely with the values obtained by Desai *et al.*,[1] and the ρ and P' trajectories are approximately exchange degenerate. The parameter values for the real parts of the three trajectories are similar to the values which have been obtained in previous real-pole fits to the πN data.[7,20]

We note that the value of g, Eqs. (8) and (9), is in the range $0.1 \lesssim g \lesssim 0.2$ for all complex-conjugate

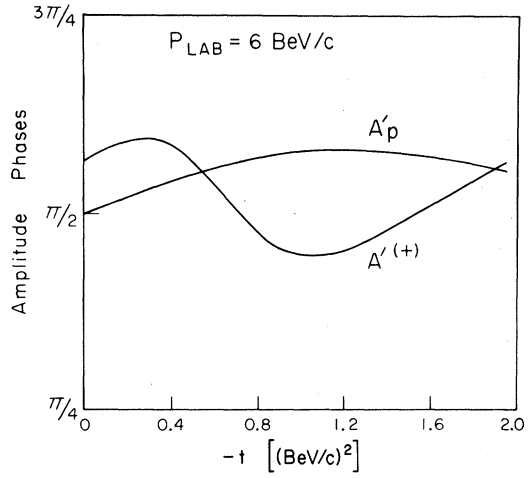

FIG. 6. Phase of $A'^{(+)}$ and A'_p at $p_{\rm lab}=6$ BeV/c. The phase remains near $\pi/2$ for all t.

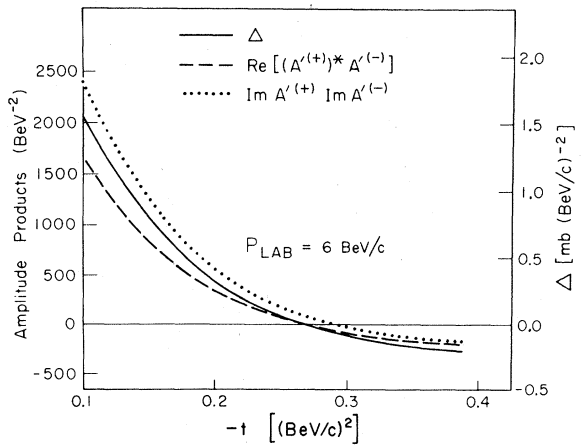

FIG. 7. $\Delta = (d\sigma/dt)(\pi^-p) - (d\sigma/dt)(\pi^+p)$, Re$[(A'^{(+)})^* A'^{(-)}]$, and Im$A'^{(+)}$ Im$A'^{(-)}$ are shown at $p_{\rm lab}=6$ BeV/c. These functions vanish at $t=-0.26$, -0.26, and -0.29 (BeV/c)^2, respectively.

trajectories. The BMZ approximation is best for small values of $\mathrm{Im}\alpha \ln(\nu/\nu_0)$, and thus it is consistent that reasonably small values of g are obtained.

(3) The crossover zero. We shall discuss the position, movement, and mechanism of production of the crossover zero in the CRP model. To do this, we define crossing even and odd amplitudes, $A'^{(+)}$ and $A'^{(-)}$, by

$$A'^{(\pm)} = \tfrac{1}{2}(A'_{\pi^- p} \pm A'_{\pi^+ p}) \tag{24}$$

with similar definitions for $B^{(+)}$ and $B^{(-)}$. We use the symbol Δ to represent the difference in the $\pi^- p$ and $\pi^+ p$ elastic cross sections,

$$\Delta = \frac{d\sigma}{dt}(\pi^- p) - \frac{d\sigma}{dt}(\pi^+ p). \tag{25}$$

According to the usual arguments,[8,19] which remain valid for complex poles, the contribution of the spin-flip amplitudes may be neglected in computing Δ, and hence

$$\Delta \sim \mathrm{Re}[(A'^{(+)})^* A'^{(-)}] = \mathrm{Im}A'^{(+)}\,\mathrm{Im}A'^{(-)} + \mathrm{Re}A'^{(+)}\,\mathrm{Re}A'^{(-)}. \tag{26}$$

For a real Pomeranchuk trajectory, $\mathrm{Re}A'_p \simeq 0$ and the approximation

$$\frac{\mathrm{Re}A'^{(+)}}{\mathrm{Im}A'^{(+)}} \simeq 0 \tag{27}$$

can be made. It follows that the zero in Δ will occur in roughly the same position as the zero in $\mathrm{Im}A'^{(-)}$.

With a complex Pomeranchuk trajectory the situation is more complicated. The approximation in Eq. (27) may or may not hold, depending on the phase of the Pomeranchuk amplitude. In the actual fits with a complex Pomeranchuk trajectory we did find that $\mathrm{Re}A'_p/\mathrm{Im}A'_p \simeq 0$. This fact is illustrated in Fig. 6 where the phases of A'_p and $A'^{(+)}$ are plotted versus $-t$ at $p_{\mathrm{lab}} = 6$ BeV/c. The phase of both amplitudes remains near $\pi/2$ for all t. These results are not surprising, since $\mathrm{Re}A'^{(+)}/\mathrm{Im}A'^{(+)}$ must be small at $t=0$ in order to agree with data on the phase of the forward amplitudes. Thus, even for P complex, $\Delta \sim \mathrm{Im}A'^{(-)}$. Of course, with either a real or complex Pomeranchuk trajectory there will be a slight difference in the position of the zeros of Δ and $\mathrm{Im}A'^{(-)}$, and this difference will depend in a complicated way on the exact model and parametrization used.

To illustrate these points explicitly, we have plotted Δ, $\mathrm{Re}[(A'^{(+)})^* A'^{(-)}]$, and $\mathrm{Im}A'^{(+)}\,\mathrm{Im}A'^{(-)}$ at $p_{\mathrm{lab}} = 6$ BeV/c in Fig. 7. The zeros of these quantities occur at $t=-0.26$, -0.26, and -0.29, respectively, and this agrees with our previous discussion.

In Fig. 8 Δ is plotted versus $-t$ for $p_{\mathrm{lab}} = 6$ and 200 BeV/c. The zero in Δ moves from $t=-0.26$ at $p_{\mathrm{lab}} = 6$ to $t=-0.47$ at $p_{\mathrm{lab}} = 200$ BeV/c. The movement of the crossover zero to larger $-t$ as p_{lab} increases is a general feature of the CRP model, as we shall now demonstrate.[22] From Eqs. (1) and (4), we obtain

$$\mathrm{Im}A' = 2\,\mathrm{Re}\left[\gamma_{+A}\left(\frac{\nu}{\nu_0}\right)^{\alpha_+}\right] = 2|\gamma_{+A}|\left(\frac{\nu}{\nu_0}\right)^{\alpha_R}\cos\left(\phi_{+A} + \alpha_I \ln\frac{\nu}{\nu_0}\right), \tag{28}$$

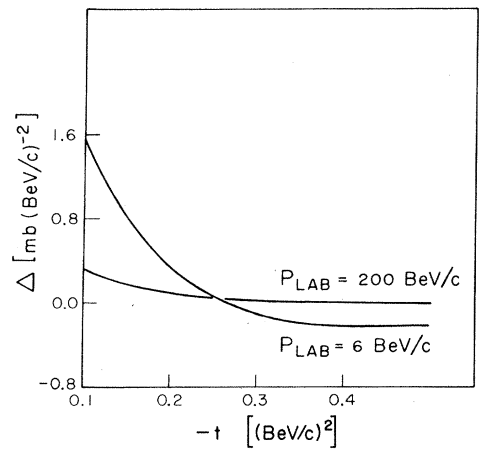

FIG. 8. $\Delta = (d\sigma/dt)(\pi^- p) - (d\sigma/dt)(\pi^+ p)$ at $p_{\mathrm{lab}} = 6$ and 200 BeV/c. The crossover zero shifts from -0.26 at 6 BeV/c to -0.47 at 200 BeV/c.

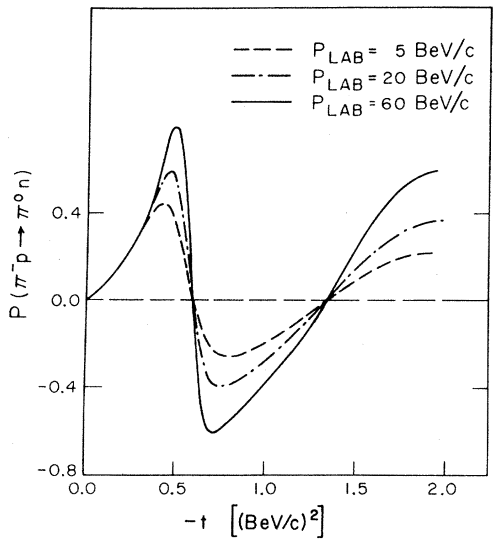

FIG. 9. Theoretical values of $P(\pi^- p \to \pi^0 n)$ at $p_{\mathrm{lab}} = 5$, 20, and 60 BeV/c.

where $\alpha_R = \mathrm{Re}\alpha$, $\alpha_I = \mathrm{Im}\alpha$, and ϕ_{+A} is the phase of γ_{+A}. Using Eq. (10), this becomes

$$\mathrm{Im}A' = 2|\gamma_{+A}|\left(\frac{\nu}{\nu_0}\right)^{\alpha_R}\cos\psi, \tag{29}$$

where

$$\psi = \phi_A + \tan^{-1}\left(\frac{\alpha_I}{\alpha_R+1}\right) + \alpha_I \ln\left(\frac{\nu}{\nu_0}\right). \tag{30}$$

The zero in $\mathrm{Im}A'$ corresponds to $\psi = -\pi/2$.[23] Thus, for fixed t, as ν increases, ψ increases and the crossover zero shifts to larger values of $-t$. There is evidence to indicate that this feature of complex Regge poles agrees with experiment.[24,25]

(4) Polarization. The new charge-exchange polarization data show a maximum of about 60% at $t \simeq -0.4$ and a zero at $t \simeq -0.6$. The CRP model fits these results very well as is evident in Fig. 2.

In Fig. 9 we have plotted the theoretical values of charge-exchange polarization at $p_{\mathrm{lab}} = 5$, 20, and 60 BeV/c to show the energy dependence in our model. We note that the maximum value of polarization near $t = -0.45$ increases and shifts to larger values of $-t$ as p_{lab} increases. We also find that the zero near $t = -0.6$ is energy-independent. This latter fact is easily understood from the energy independence of the term $\sin[\phi_B - \phi_A + \arg(\alpha_+)]$ which is responsible for the vanishing of polarization in our model. Unfortunately, the data are not sufficiently accurate to test these characteristics of the fit.

The CRP model agrees fairly well with the new elastic polarization data, although there is a small difference between theory and experiment in the $\pi^+ p$ data at $p_{\mathrm{lab}} = 6$ BeV/c.

The elastic polarization $P(\pi^\pm p)$ is given by the equation[8]

$$P(\pi^\pm p) = -\frac{\sin\theta_s}{16\pi s^{1/2}}\frac{\mathrm{Im}(A'_{\pi^\pm p}B^*_{\pi^\pm p})}{(d\sigma/dt)(\pi^\pm p)}. \tag{31}$$

Combining this relation with (24), we obtain

$$P(\pi^\pm p) = \mp P_0(\pi^\pm p) + P_1(\pi^\pm p), \tag{32}$$

where P_0 and P_1 are defined by

$$P_0(\pi^\pm p) = -\frac{\sin\theta_s}{16\pi s^{1/2}} \times \frac{\mathrm{Im}[A'^{(+)}B^{(-)*}] + \mathrm{Im}[A'^{(-)}B^{(+)*}]}{(d\sigma/dt)(\pi^\pm p)}, \tag{33}$$

$$P_1(\pi^\pm p) = -\frac{\sin\theta_s}{16\pi s^{1/2}} \times \frac{\mathrm{Im}[A'^{(+)}B^{(+)*}] + \mathrm{Im}[A'^{(-)}B^{(-)*}]}{(d\sigma/dt)(\pi^\pm p)}. \tag{34}$$

Since $(d\sigma/dt)(\pi^+ p) \simeq (d\sigma/dt)(\pi^- p)$, it follows that $P_0(\pi^+ p) \simeq P_0(\pi^- p)$ and $P_1(\pi^+ p) \simeq P_1(\pi^- p)$, and we may now use P_0 and P_1 to discuss the symmetry characteristics of the polarization data.

In Fig. 5 it is evident that the data show an approximate mirror symmetry, that is $P(\pi^+ p) \simeq -P(\pi^- p)$, and therefore we expect that P_0 will dominate over P_1 in any model which fits the data. This is verified for the CRP model in Fig. 10 where the contributions of P_0 and P_1 to the elastic $\pi^- p$ polarization at $p_{\mathrm{lab}} = 6$ BeV/c are plotted.

The polarization does show some asymmetry which cannot be ignored in an accurate fit. For small $-t$, $|t| \lesssim 0.6$, the magnitude of $P(\pi^+ p)$ is generally a little larger than the magnitude of $P(\pi^- p)$. For larger $-t$ the asymmetry is reversed: $|P(\pi^- p)| > |P(\pi^+ p)|$. However, there are large uncertainties in the experimental results for $|t| > 0.8$, and the exact degree of asymmetry is poorly determined. From Fig. 10 we note that $P_1 > 0$ for $|t| < 0.8$ and $P_1 < 0$ for $|t| > 0.8$, which is consistent with the above discussion.

In P_1 there are terms which result from the interference of a Regge pole with itself, namely, $\mathrm{Im}(A'_p B^*_p)$, $\mathrm{Im}(A'_{p'} B^*_p)$, and $\mathrm{Im}(A'_\rho B^*_\rho)$. Although these terms vanish identically for real poles, they may result in significant nonzero polarization with complex poles and residues. This fact has already been demonstrated in charge-exchange scattering where the entire polarization results from ρ-ρ interference. However, the fitting program has adjusted the trajectories and residues in such a way that the value of P_1 remains fairly small and is consistent with the data.

In general, either large or small contributions from terms involving the interference of a pole with itself are possible and the CRP model pro-

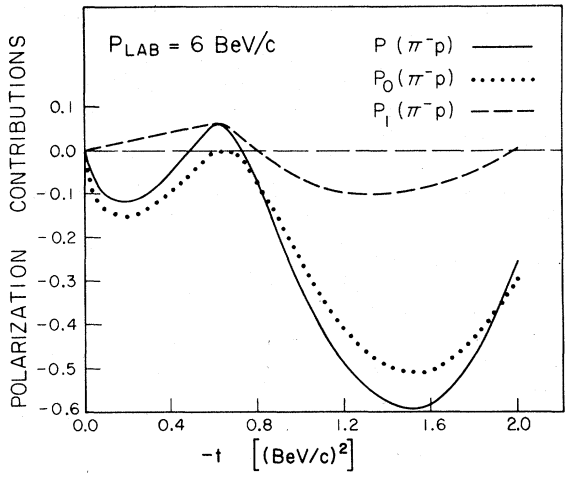

FIG. 10. P_0, P_1, and P for $\pi^- p$ elastic scattering at $p_{\mathrm{lab}} = 6$ BeV/c. These quantities are defined in Eqs. (31)–(34).

vides a high degree of flexibility in fitting polarization data that is not available in real-pole models.

The double-zero structure of the elastic polarization near $t=-0.6$ may be explained as follows. For t small, $|A'^{(+)}| \gg |A'^{(-)}|$. Combining this with Eq. (27) and the approximate mirror symmetry of the data, we obtain

$$P(\pi^{\pm}p) \simeq \mp P_0(\pi^{\pm}p) \sim \pm \mathrm{Im}\, A'^{(+)}\, \mathrm{Re}B^{(-)}. \quad (35)$$

Since $\mathrm{Re}B^{(-)}$ has a double zero in our model, we should expect that P_0, and hence $P(\pi^{\pm}p)$, will show approximately the same structure. This explanation of the double zero agrees with the usual real-pole analysis.[7]

(5) Concluding remarks. We have shown that the CRP model provides excellent fits to the πN charge-exchange and elastic scattering data. We have discussed the detailed features of complex Regge poles in πN scattering and have observed that the data show no strong preference for either a real or complex-conjugate Pomeranchuk trajectory or for a logarithmic or square-root branch cut.

ACKNOWLEDGMENTS

The authors are grateful to Dr. B. R. Desai, Dr. P. Kaus, Dr. R. J. N. Phillips, and Dr. V. A. Tsarev for useful discussions. One of us (R.T.P.) would like to thank Dr. G. Chew for his hospitality at the Lawrence Radiation Laboratory where part of this work was carried out.

---

*Work supported in part by the National Science Foundation.

†Present address: Department of Physics and Astronomy, California State University, Northridge, California 91324.

‡Address after September 1, 1972: Department of Physics, Utkal University, Bhubaneswar-4, Orissa, India.

[1]B. R. Desai, P. Kaus, R. T. Park, and F. Zachariasen, Phys. Rev. Letters 25, 1389; 25, 1686(E) (1970).

[2]N. Barik, B. R. Desai, P. Kaus, and R. T. Park, Phys. Rev. D 4, 2923 (1971).

[3]O. Guisan *et al.*, Saclay-Orsay-DESY-Paris Collaboration, 1971 (unpublished).

[4]M. Borghini *et al.*, Phys. Letters 31B, 405 (1970); M. Borghini *et al.*, report submitted to the Fifteenth International Conference on High Energy Physics, Kiev, U.S.S.R., 1970 (unpublished); and G. Bellettini (private communication).

[5]N. Barik and B. R. Desai, Phys. Rev. D 6, 3192 (1972). The authors have reviewed the evidence for this statement and give further references.

[6]J. S. Ball, G. Marchesini, and F. Zachariasen, Phys. Letters 31B, 383 (1970).

[7]V. Barger and R. J. N. Phillips, Phys. Rev. Letters 22, 116 (1969).

[8]W. Rarita, R. J. Riddell, Jr., C. B. Chiu, and R. J. N. Phillips, Phys. Rev. 165, 1615 (1968).

[9]C. B. Chiu, S. Y. Chu, and L. L. Wang, Phys. Rev. 161, 1563 (1967).

[10]A. V. Stirling *et al.*, Phys. Rev. Letters 14, 763 (1965); P. Sonderegger *et al.*, Phys. Letters 20, 75 (1966).

[11]P. Bonamy *et al.*, Phys. Letters 23, 501 (1966).

[12]K. J. Foley *et al.*, Phys. Rev. Letters 19, 330 (1967).

[13]K. J. Foley *et al.*, Phys. Rev. Letters 19, 193 (1967).

[14]K. J. Foley *et al.*, Phys. Rev. Letters 11, 425 (1963); D. Harting *et al.*, Nuovo Cimento 38, 60 (1965).

[15]C. T. Coffin *et al.*, Phys. Rev. 159, 1171 (1967).

[16]M. Borghini *et al.*, Phys. Letters 24B, 77 (1966).

[17]Unless otherwise specified, the theoretical curves in all figures in this paper will be calculated on the basis of the $\chi^2=761$ parameters – cyclic residue, complex Pomeranchuk trajectory, and square-root branch cut. This is done for simplicity in presenting the results. We note that the difference in quality between the $\chi^2=761$ fits and the fits for other values of χ^2 in Table II is not substantial, and the fundamental results are the same in all cases. This point is discussed in further detail in the text.

[18]V. A. Tsarev and N. P. Zotov, Sov. J. Nucl. Phys. 14, 806 (1971); O. Sugikchasi, S. V. Tarasevitch, V. A. Tsarev, and N. P. Zotov, P. N. Lebedev Physical Inst. Brief Communications in Physics 9, 53 (1971).

[19]R. J. N. Phillips and W. Rarita, Phys. Rev. 139, B1336 (1965).

[20]V. Barger and R. J. N. Phillips, Phys. Rev. 187, 2210 (1969).

[21]J. N. J. White, Nucl. Phys. B13, 139 (1969).

[22]The CRP model is not unique in this respect. We have found that the zero in Δ in the real-pole fits of Ref. 20 moves from $t\simeq -0.15$ at $p_{\mathrm{lab}}=6$ BeV/c to $t\simeq -0.23$ at $p_{\mathrm{lab}}=200$ BeV/c.

[23]The arguments which show that $\psi=-\frac{1}{2}\pi$ and not, for example, $+\frac{1}{2}\pi$ are given in Ref. 2.

[24]B. R. Desai, Phys. Rev. D 4, 3321 (1971).

[25]F. Halzen and C. Michael, Phys. Letters 36B, 367 (1971).